Science of the Total Environment 738 (2020) 139908

Contents lists available at ScienceDirect

Science of the Total Environment

journal homepage: www.elsevier.com/locate/scitotenv

Black carbon-enhanced transformation of dichloroacetamide safeners: Role of reduced sulfur species

Xiaolei Xu [a], John D. Sivey [b], Wenqing Xu [a,*]

[a] Department of Civil and Environmental Engineering, Villanova University, Villanova, PA 19085, USA
[b] Department of Chemistry, Towson University, Towson, MD 21252, USA

HIGHLIGHTS

- Complete dechlorination of all (di) chloroacetamides was observed.
- Polysulfides are likely to account for the observed accelerated transformation of (di)chloroacetamides.
- Di- and/or trimerization of (di) chloroacetamides is anticipated to decrease the mobility of transformation products relative to parent compounds.

GRAPHICAL ABSTRACT

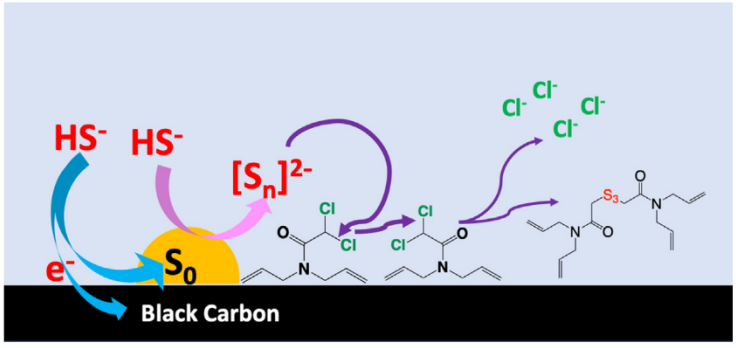

ARTICLE INFO

Article history:
Received 17 April 2020
Received in revised form 27 May 2020
Accepted 31 May 2020
Available online 02 June 2020

Editor: Jay Gan

Keywords:
Halogenated agrochemical fate
Nucleophilic dechlorination
Polysulfides
Subsurface environments

ABSTRACT

Dichloroacetamide safeners are commonly included in herbicide formulations to protect crops from unintended herbicide toxicity, but knowledge of their environmental fate is scarce. Hydrogen sulfide, a naturally-occurring nucleophile and reductant, often coexists with black carbon (*e.g.*, biochar, soot) in subsurface environments and could influence the fate of these safeners. In this study, we demonstrated that graphite powder, a model black carbon, significantly accelerated the transformation of three dichloroacetamide safeners (AD-67, benoxacor, and dichlormid) and two chloroacetamide herbicides (metolachlor and acetochlor) by hydrogen sulfide. Chloride was formed together with an array of sulfur-substituted products, suggesting a nucleophilic substitution pathway. Our results suggest that the electron-accepting capacity of black carbon can oxidize hydrogen sulfide species to elemental sulfur, which can further react with bisulfide to form polysulfide, likely accounting for the observed accelerated transformation of (di)chloroacetamides in systems containing black carbon and hydrogen sulfide. Moreover, our product analyses indicate that dimerization and/or trimerization of (di) chloroacetamides is possible in the presence of hydrogen sulfide and graphite, which is anticipated to decrease the mobility of these products in aquatic environments relative to the parent compounds. Herein, we also discuss how the structure and concentration of (di)chloroacetamides can influence their reactivity in the presence of black carbon and reduced sulfur species.

1. Introduction

Safeners are chemicals commonly included in herbicide formulations to protect crops from injury following exposure to herbicides (Rosinger et al., 2011). Since their first commercial application in

* Corresponding author.
E-mail address: wenqing.xu@villanova.edu (W. Xu).

https://doi.org/10.1016/j.scitotenv.2020.139908
0048-9697/

1971, approximately twenty safeners have been developed (Abu-Qare and Duncan, 2002; Jablonkai, 2013). Dichloroacetamides are among the most commonly used safeners and have an estimated annual usage of ~2 × 10^6 kg in the United States (Abu-Qare and Duncan, 2002; Jablonkai, 2013; Rosinger et al., 2011Sivey and Roberts, 2012). Dichloroacetamide safeners such as benoxacor, dichlormid, and AD-67 are routinely used in corn production and are often paired with either a chloroacetamide (*e.g.*, metolachlor or acetochlor) or thiocarbonate herbicide. Typically, dichloroacetamide safeners contribute up to ~5 wt% of the herbicide formulation (Jablonkai, 2013; Sivey et al., 2015; Sivey and Roberts, 2012). However, environmental fate data for safeners are scarce (Kral et al., 2019; Sivey et al., 2015; Sivey and Roberts, 2012; Su et al., 2019), possibly resulting from their regulatorily classification as "inert" ingredients (Davies and Caseley, 1999).

Considering the fact that dichloroacetamide safeners have been co-applied with herbicides at comparable rates for decades (Abu-Qare and Duncan, 2002), it is likely that these safeners are present in a range of environmental systems, particularly those proximate to agricultural lands. Moreover, many dichloroacetamide safeners have lower K_{ow} values (1.8 to 2.7) and similar half-lives (DT_{50}) in soil relative to chloroacetamide herbicides (Acharya and Weidhaas, 2018; Bolyard et al., 2017; Loch et al., 2002; Sivey et al., 2015; Sivey and Roberts, 2012). The fact that companion herbicides have been frequently detected in various environmental compartments (*e.g.*, surface water (Hladik et al., 2005), soil (Aga et al., 1996), ground water (Kolpin et al., 1998), and drinking water (Hladik et al., 2008)) suggests that safeners are highly likely to be present in these systems. In fact, concentrations up to 190 ng/L of AD-67, benoxacor, and dichlormid have been reported in Midwestern U.S. streams (Woodward et al., 2018). In addition, although safeners have been detected at somewhat lower concentrations in surface waters (~ng/L), dichlormid has been detected at much higher concentrations on soil surfaces (0.01–0.02 mg/kg) 21 days after application (Wilson and James, 1987). The presence of one additional (geminal) chlorine atom is anticipated to make dichloroacetamide safeners less likely to be metabolized by plants (Scarponi et al., 1991) and soil bacteria (Feng, 1991). Collectively, these observations suggest that safeners are likely to percolate through soil and enter the subsurface environment, where iron minerals, black carbon, and hydrogen sulfide are abundant. Benoxacor is highly toxic to aquatic autotrophs such as freshwater algae (European Chemicals Agency, 2020) and is also moderately toxic to aquatic animal species such as freshwater fish, *Ictalurus punctatus* (US EPA, 2020). Dichloroacetamide safeners display generally low mammalian toxicity but some studies indicate that they are potentially carcinogenic and/or mutagenic to rats (Coleman et al., 2000; Kale et al., 2008; Klopman et al., 2003). Yet, little is known regarding the fate of dichloroacetamide safeners in subsurface environments. Although the reductive dechlorination of dichloroacetamide safeners by surface-adsorbed Fe(II) species has been reported (Sivey and Roberts, 2012), the impact of other environmental reagents, such as hydrogen sulfide and black carbon, has not been examined.

Hydrogen sulfide naturally exists at concentrations up to 5 mM under anaerobic conditions (Dunnette et al., 1985; King et al., 1982) and can transform various agrochemicals including (mono) chloroacetamide herbicides (*e.g.*, metolachlor) (Christian et al., 2018; Loch et al., 2002; Wu et al., 2006; Zeng et al., 2013). However, the fate of dichloroacetamides in the presense of hydrogen sulfide has not been previously investigated. Black carbon (*e.g.*, biochar, soot), the solid residue from the incomplete combustion of fossil fuel or biomass, is ubiquitous in the environment and typically constitutes 1–20% of the total organic carbon in soils and sediments (Ding et al., 2018; Lian and Xing, 2017; Middelburg et al., 1999; Pignatello et al., 2017), corresponding to concentrations of 1.25–25 g·L^{-1} (Xu et al., 2010). Black carbon often coexists with hydrogen sulfide. Recent studies suggest a synergy between black carbon and hydrogen sulfide in promoting contaminant transformation (*e.g.*, 1,1,1-trichloro-2,2-di(4-chlorophenyl)ethane (DDT), nitroaromatics) (Ding and Xu, 2016; Kemper et al., 2008; Xu et al., 2010; Xu et al., 2013; Xu et al., 2015). Several reaction mechanisms have been proposed for this synergy. Specifically, black carbon could increase rates of contaminant transformation by: (1) accelerating electron transfer from hydrogen sulfide to adsorbed contaminants; (2) promoting conversion of hydrogen sulfide into reactive surface-bound nucleophiles; and/or (3) oxidizing hydrogen sulfide to other reactive sulfur species (*e.g.*, polysulfide) (Ding and Xu, 2016; Kemper et al., 2008; Xu et al., 2010; Xu et al., 2013; Xu et al., 2015). Nevertheless, possible synergies between black carbon and hydrogen sulfide on the transformation of (di)chloroacetamide agrochemicals has not been investigated despite the fact that (di)chloroacetamides are anticipated to be more mobile in the subsurface compared to DDT and nitroaromatics (Ding and Xu, 2016; Xu et al., 2015).

The goals of the current study include: (1) characterizing the transformation kinetics and products of three dichloroacetamide safeners (AD-67, benoxacor, and dichlormid) and, as a point of comparison, chloroaceteamide herbicides (metolachlor and acetochlor), upon reaction with hydrogen sulfide in the presence and absence of a model black carbon (graphite); (2) investigating the putative reaction mechanism(s) associated with these transformations; and (3) evaluating the properties of black carbon that are influential in promoting the transformation of (di)chloroacetamides.

2. Materials and methods

2.1. Chemical reagents

Detailed information for chemicals is provided in the Supporting Information (SI, Text S1). Unless otherwise specified, all reduced sulfur solutions were prepared in MOPS buffer (10 mM, pH 7.2 ± 0.1) that was previously purged with N_2 for 2 h and stored in a glovebox (5% H_2, 20% CO_2, 75% N_2, Coy Laboratory Product Inc.) to ensure anaerobic conditions (O_2 < 5 ppm). *TOT*HS (total hydrogen sulfide), referred to the sum of H_2S, HS^-, and S^{2-}, stock solutions were freshly prepared by dissolving $Na_2S·9H_2O$ in MOPS buffer. Polysulfide (S_n^{2-}) solution was prepared using a method adapted from the literature (Lippa and Roberts, 2002): an aliquot (0.8 mL) of aqueous supernatant from a mixture containing excess elemental sulfur (S_8, 7.5 mM) and *TOT*HS (60 mM) was diluted to a final volume of 9 mL with MOPS buffer. The solution was subsequently equilibrated for a week and analyzed for *TOT*HS, S_8^-, and S_n^{2-}, which were determined to be 5 mM, 1 mM, and 300 μM by sulfur atom, respectively. Polysulfide concentration was reported as the total sulfur atom on a molar basis in polysulfide.

2.2. Batch reactor experiments

Graphite powder was selected as a model black carbon due to its high carbon content (~99.99% by weight) and lack of surface functionalites. Samples were prepared in 14-mL borosilicate vials containing pre-weighed graphite powder (21 g·L^{-1}). MOPS buffer was added into the vials to fill up approximately 80% of the volume. *TOT*HS stock solution was added to achieve a final concentration of 5 mM. Stock solutions (200 μL) of AD-67, benoxacor, dichlormid, metolachlor, and acetochlor (2 mM in acetonitrile) were then spiked into the system to yield an initial (di)chloroacetamide concentration of 21–28 μM. The headspace was then eliminated by adding MOPS buffer to the top. All samples were capped with Teflon-lined septa, vortexed to mix for 3 min, and then placed on an end-to-end rotator (Glas-Col) in the dark at 30 rpm and 25 °C in an incubator (VWR International). Controls with 21 g·L^{-1} graphite in the absence of *TOT*HS, 5 mM *TOT*HS in the absence of graphite, and in the absence of both *TOT*HS and graphite were also performed. Biochar experiments for dichlormid were conducted using the same protocol with a biochar loading of 10 g·L^{-1}. The maximum duration of kinetics experiments for AD-67, benoxacor,

dichlormid, acetochlor and metolachlor was 114, 120, 72, 8, and 96 h, respectively.

2.3. Electrochemical cells experiments

Electrochemical cells were set up following the same protocol as described in our previous publications (Ding and Xu, 2016; Xu et al., 2015). Briefly, two 24-mL borosilicate glass vials were connected *via* an insulated copper wire through Teflon-lined septa. Graphite sheets (0.13 mm thickness; Alfa Aesar) were used as the cathode and anode, which were attached to the copper wire with conductive NEM tape (Nisshi EMCO Ltd). The electrical circuit was completed using a salt bridge containing 1 M K_2SO_4 in Teflon tubing. *TOT*HS was spiked into the anodic cell at an initial concentation of 5 mM. (Di)chloroacetamides were introduced to the cathodic cell at initial concentrations of 21–28 μM. Periodically, the cathodic cells were sampled. Both the aqueous and solid phases were analyzed for (di)chloroacetamides as described below.

2.4. TOTHS-pretreated graphite experiments

To facilitate the reaction between graphite and *TOT*HS, pre-weighed graphite powder (21 $g \cdot L^{-1}$) in 14-mL borosilicate vials was exposed to 5 mM *TOT*HS in headspace-free vials containing MOPS buffer. After 24 h, samples were centrifuged and the aqueous phase was decanted. The solid phase was rinsed twice with 10 mL MOPS buffer to remove residual *TOT*HS; the *TOT*HS concentration was measured in each wash (Fig. S1). After rinsing the graphite twice, the residual *TOT*HS concentration was <2 μM. Subsequently, vials containing the *TOT*HS-pretreated graphite were refilled with MOPS buffer and (di)chloroacetamides (200 μL at 2 mM in acetonitrile) were spiked into the system to initiate the reaction.

2.5. Bulk electrolysis of (di)chloroacetamides

Bulk electrolysis of (di)chloroacetamides was performed to determine whether they can be directly reduced under environmentally-relevant reduction potentials (*i.e.*, $HS^- \rightarrow S_0 + H^+ + 2e^-$, $E_H = -0.47$ V). Experiments were conducted using a potentiostat (600E, CH Instruments) in a glove box. A voltammetry cell was set up with a glassy carbon working electrode, an Ag/AgCl reference electrode, and a platinum wire counter electrode (BASi, Inc). Reduction potentials (E) were measured against Ag/AgCl reference electrode and are reported relative to the standard hydrogen electrode (E_H). (Di)chloroacetamides were spiked into the voltammetry cell to achieve initial concentrations of 21–28 μM. Electrochemical reduction was initiated by applying an $E_H = -0.47$ V; the reductive current was continuously monitored. Reduction was terminated after 48 h when the reductive current had returned to the background current value (2.2×10^{-6} A), which was independently determined for the same solutions (10 mM phosphate buffer, pH 7) but in the absence of (di)chloroacetamides. Solutions in the voltammetry cell were sampled for (di)chloroacetamide analyses as described below.

2.6. Electrochemcial reduction of graphite

Graphite powder was electrochemically reduced using a potentiostat (600E, CH Instruments) in a glove box to deplete its electron-accepting capacity (EAC). The electrochemical reduction was initiated by applying an $E_H = -0.55$ V to a voltammetry cell containing pre-weighed graphite powder (45 $g \cdot L^{-1}$) with the same three-electrode set-up. This reduction potential was chosen because it is lower than the two-electron reduction potential of bisulfide ($E_H = -0.47$ V), which was assumed to be sufficient in reducing the EAC of graphite. The reaction was terminated after 24 h when the reductive current returned to the background current value (2.2×10^{-6} A). Subsequently, the reduced graphite powder was washed with 40 mL MOPS buffer (10 mM) twice and allowed to dry in the glove box.

2.7. Biochar preparation and characterization

Oak wood was used to produce biochar *via* slow pyrolysis in a tube furnace (Model 1600, CM Inc.) at 400, 500, 600, and 700 °C under N_2 (50 $mL \cdot min^{-1}$). The furnace was ramped up to the desired temperature at 5 $°C \cdot min^{-1}$, held for 2 h, and cooled to room temperature. Elemental analysis of black carbon was performed by Galbraith Laboratories (PerkinElmer 2400 CHNS/O Series II; Thermo Scientific FlashEA 1112) and surface area was characterized by N_2 sorption (NOVA 3000e, Quantachrome Instruments) (Table S1). The electrical conductivity of all black carbon was measured using a two-probe bed technique (Text S2 and Fig. S13) (Avetisyan et al., 2019).

The EAC values of chars were measured by a modified back titration method (Li et al., 2019; Matsumura and Takahashi, 1979). Briefly, excess $NaBH_4$ (0.025 M) was added to reduce samples containing biochar (2 $g \cdot L^{-1}$) in NH_4Cl-NH_4OH buffer (0.2 M; pH 10). I_2 (0.045 M) was then added to oxidize samples. Redox potentials (E_H) were recorded against the volume of added titrant (Fig. S2A). Meanwhile, one blank sample without biochar was set up. Experiments were conducted in the dark under N_2. EAC values were calculated based on the differences in I_2 consumption between samples and the blank at −456 mV, assuming an 8-electron oxidation of $NaBH_4$ and a 2-electron reduction of I_2 at pH 10.

2.8. Chemical analysis

For homogeneous systems, reactor aliquots (1 mL) were withdrawn and analyzed directly. For heterogeneous systems, reaction vials were centrifuged (Forma Scientific 5678) at 3000 rpm for 3 min. Solid phases were extracted by shaking with 5.0 mL acetonitrile for 3 min. Solid-phase extraction efficiencies for AD-67, benoxacor, dichlormid, metolachlor, and acetochlor from graphite were 88 ± 1%, 94 ± 1%, 92 ± 1%, 93 ± 1%, and 107 ± 3%, respectively. Solid phase extraction efficiencies for dichlormid from the biochar prepared at 400, 500, 600, and 700 °C were 78 ± 1%, 72 ± 1%, 84 ± 1%, and 84 ± 2%, respectively. Both aqueous and solid phase-extracts were analyzed for (di) chloroacetamides using a Shimadzu HPLC-UV; instrumental method details are provided in Table S2. Chloride ion was analyzed by an ion chromatograph coupled with a conductivity detector (CDD-10A, Shimazu) at 45 °C with 3.6 mM Na_2CO_3 as the mobile phase at a flow rate of 0.8 $mL \cdot min^{-1}$. *TOT*HS was quantified colorimetrically (Cline, 1969). Elemental sulfur was quantified by HPLC-UV (Table S2), where the aqueous phase was analyzed directly and the solid phase was extracted using neat dichloromethane (McGuire and Hamers, 2000; Zheng et al., 2015). Polysulfides were quantified by a modified gas chromatography-mass spectroscopy (GC–MS) method after reacting with methyl iodide to form dimethyl-polysulfanes (Goifman et al., 2004; Kristiana et al., 2010; Zeng et al., 2011). The method converts various polysulfide ions into dimethyl-polysulfanes measurable by GC–MS based on the following reactions:

$$HS^- + \frac{(n-1)}{8} S_8 \rightleftharpoons H^+ + S_n^{2-}$$

$$S_n^{2-} + 2CH_3I \rightarrow CH_3S_nCH_3 + 2I^-$$

Specifically, 1.00-mL supernatant or slurry was mixed with 200 μL neat methyl iodide (≈ 2 M) in a glove box and heated to 60 °C in a water bath for 1 h. The mixture was then cooled to room temperature and extracted with 0.50 mL *n*-hexane. The extracts were analyzed by GC–MS; instrumental method details including the elution time of dimethyl- disulfide, trisulfide, and tetrasulfide standards are provided in Table S3. Although polysulfide anions are mainly in the form of

pentasulfide and tetrasulfide anions in water (Kamyshny et al., 2007), we have observed only dimethyl disulfide and dimethyl trisulfide in methylated samples (Fig. S2B). This is possibly due to the rearrangement of sulfur chain during the methylation process (Zeng et al., 2011). We ackowledge that the method may not be able to differentiate individual polysulfide species (Goifman et al., 2004; Zeng et al., 2011). Therefore, we reported polysulfide concentrations as the sum of the sulfur atom in dimethyl disulfide and dimethyl trisulfide species (Zeng et al., 2011).

Ultra-performance liquid chromatography (UPLC) interfaced with a high-resolution, quadrupole/time-of-flight mass spectrometer (qTOF-MS) was employed to analyze organic transformation products in aqueous and solid phase-extracts of selected systems. Additional UPLC-qTOF-MS methodological details are provided in the SI (Text S3) and Fig. S3.

3. Results and discussion

3.1. Transformation kinetics of (di)chloroacetamide safeners and herbicides

As shown in Fig. 1A, no appreciable loss of AD-67 was observed over 120 h in controls containing MOPS buffer with and without graphite powder, indicating that neither hydrolysis nor irreversible adsorption of AD-67 ensued on this timescale. In contrast, AD-67 transformation occurred in samples containing *TOT*HS, with an observed pseudo-first-order rate constant (k_{obs}) of 0.0053 ± 0.0003 h^{-1}, corresponding to a half-life ($t_{1/2}$) of 130 ± 6 h. Unless otherwise indicated, uncertainties herein denote standard deviations of experimental duplicates. The presence of graphite powder accelerated the transformation of AD-67 by *TOT*HS, with $t_{1/2}$ shortened to 27.0 ± 0.7 h. Similar results were observed for benoxacor (Fig. 1B), metolachlor (Fig. 1C), and acetochlor (Fig. 1D) where the $t_{1/2}$ decreased in the presence of graphite powder from 100 ± 7 h to 11.3 ± 0.6 h, from 35.5 ± 0.7 h to 20.0 ± 0.4 h, and from 2.4 ± 0.2 to 1.4 ± 0.2, respectively. The decay of dichlormid by *TOT*HS (Fig. 1E) was too slow to quantify over 144 h. However, the presence of graphite powder accelerated dichlormid decay ($t_{1/2}$ = 10 ± 1 h). All values of k_{obs} and $t_{1/2}$ for (di)choloroacetamide are summarized in Table S4. Taken together, these results suggest a synergistic effect on the transformation of these (di)choloroacetamide agrochemicals when *TOT*HS and graphite co-exist.

For reactions of (di)chloroacetamides in homogenous systems containing *TOT*HS, k_{obs} decreased in the order of acetochlor (k_{obs} = 0.29 ± 0.03 h^{-1}) > metolachlor (k_{obs} = 0.0195 ± 0.0007 h^{-1}) > benoxacor (k_{obs} = 0.0065 ± 0.0002 h^{-1}) > AD-67 (k_{obs} = 0.0053 ± 0.0003 h^{-1}) > dichlormid (too slow to quantify). Previous studies suggest that the reaction between metolachlor and *TOT*HS followed a bimolecular nucleophilic substitution pathway (S_N2), where bisulfide attacked the electrophilic C of the C—Cl bond, thereby displacing Cl^- (Loch et al., 2002; Mora et al., 2018). Acetochlor degradation by *TOT*HS was faster than metolachlor, consistent with previous results (Zeng et al., 2011) which can be ascribed to the greater steric hindrance imparted by the R-group on the nitrogen of metolachlor. Assuming that dichloroacetamide safeners follow the same reaction pathway, the lower reactivity of benoxacor compared to metolachlor could be attributed to the presence of an additional (geminal) chlorine atom, which can impart steric hindrance to nucleophilic attack on the associated carbon atom. The three safeners ($Cl_2CHC(=O)NRR'$) differ from each other in their R groups. Accordingly, we postulate that the observed reactivity trend (benoxacor > AD-67 > dichlormid) predominately results from differing steric effects imparted by the R-groups. Specifically, cyclic R-groups (benoxacor and AD-67) are anticipated to exert less steric hindrance because they have less rotational freedom and are further removed from the dichloroacetyl group compared to the more flexible allyl groups of dichlormid. Moreover, π-electrons in the R-group connected to the amide group could conceivably donate electron density *via* a through-space (field) effect and thereby stabilize the transition state as the reactive carbon atom accumulates positive charge and thereby increase its reactivity (benoxacor > AD-67) (Lippa et al., 2004; Saburo, 1952). Our results differ from a previous study where reduction rates of dichloroacetamide safeners (AD-67 > dichlorimid > benoxacor) were investigated in homogenous solutions of Cr(II) (Sivey and Roberts, 2012). Such divergence could result from differences in reaction mechanism. For example, steric hindrance may slow down S_N2 reactions, but steric effects are less important for reductive dechlorination involving dissolved reactants (Anslyn and Dougherty, 2005; Moelwyn-Hughes, 1971; Sivey and Roberts, 2012)

In contrast to homogeneous solutions of *TOT*HS, heterogeneous systems containing both *TOT*HS and graphite powder followed a different trend of reactivity: acetochlor (k_{obs} = 0.50 ± 0.07 h^{-1}) > dichlormid (k_{obs} = 0.067 ± 0.004 h^{-1}) ≈ benoxacor (k_{obs} = 0.061 ± 0.004 h^{-1}) > metolachlor (k_{obs} = 0.034 ± 0.004 h^{-1}) > AD-67 (k_{obs} = 0.026 ± 0.002 h^{-1}). Ratios of k_{obs} values from the heterogeneous system to those of the homogeneous system reflect the enhancement factor by graphite powder, which followed the order of dichlormid (>200) > benoxacor (8.8 ± 0.9) > AD-67 (4.8 ± 0.4) > metolachlor (1.7 ± 0.1) ≈ acetochlor (1.7 ± 0.3). Notably, mass transfer processes appear to have a negiligible effect on the reaction kinetics due to the fast adsorption kinetics (Fig. S4). We therefore postulate that the observed differences in graphite-enhanced reactivities result from variable interactions between (di)chloroacetamides and graphite, potentially including cavity effect, dispersion forces, and other specific interactions between the (di)chloroacetamides and graphite. The presence of π-electrons and the planarity of the aromatic ring in benoxacor could contribute to a stronger interaction with graphite surfaces (Keiluweit and Kleber, 2009), which might change the conformation of the adsorbed molecules and thereby render the reaction sites more accessible to the nucleophile and/or increase the local concentration of benoxacor (reactivity: benoxacor > AD-67). However, the associate reaction pathways might differ between the homonegous and heterogenous systems, which are explored below.

3.2. Identification of transformation products

Reactions of AD-67, benxacor, dichlormid, metolachlor, and acetochlor with *TOT*HS in the presence of graphite powder generated chloride (Fig. 2). At the end of 72 h, 18 μM of AD-67 was degraded while 31 μM of chloride was formed, and the molar yield of chloride (as Δ[Cl^-]/Δ[(di)chloroacetamide]) was 1.7 ± 0.2. The molar yield of chloride (at last sample point) from benoxacor, dichlormid, metolachlor, and acetochlor was 1.8 ± 0.2, 1.7 ± 0.1, 1.2 ± 0.2, and 1.1 ± 0.3, respectively. The mass balance on total chlorine, calculated as the ratio of (2[dichloroacetamide] + [monochloroacetamide] + [Cl^-])/(2[dichloroacetamide]$_0$ + [monochloroacetamide]$_0$), was 86%, 83%, 87%, 115%, and 113% for AD-67, benoxacor, dichlormid, metolachlor, and acetochlor, respectively, indicating a nearly complete displacement of chlorine. Furthermore, we investigated the possible formation of monochloro- and deschloro-hydrogenolysis products during transformation of (di)chloroacetamides (Table S2). However, none of these products were detected.

To characterize organic transformation products, UPLC-qTOF-MS analyses were performed. In heterogeneous systems containing graphite powder and *TOT*HS, bisulfide/hydrogen sulfide displaced all chlorine atoms of the (di)chloroacetamides. Transformation of AD-67, benoxacor, metolachlor, and acetochlor all formed almost exclusively (multi)sulfur-bridged dimers while AD-67 and acetochlor also generated (multi)sulfur-bridged trimers (Tables 1 and S5). Dichlormid yielded cyclization products in addition to (multi)sulfur-bridged dimers. Similarly, in homogeneous systems containing *TOT*HS, AD-67, metolachlor, and acetochlor generated sulfur-substituted products containing no chlorine atoms. However, no identifiable products were detected for benoxacor and dichlormid in systems containing only *TOT*HS. Details on the characterized transformation products, their

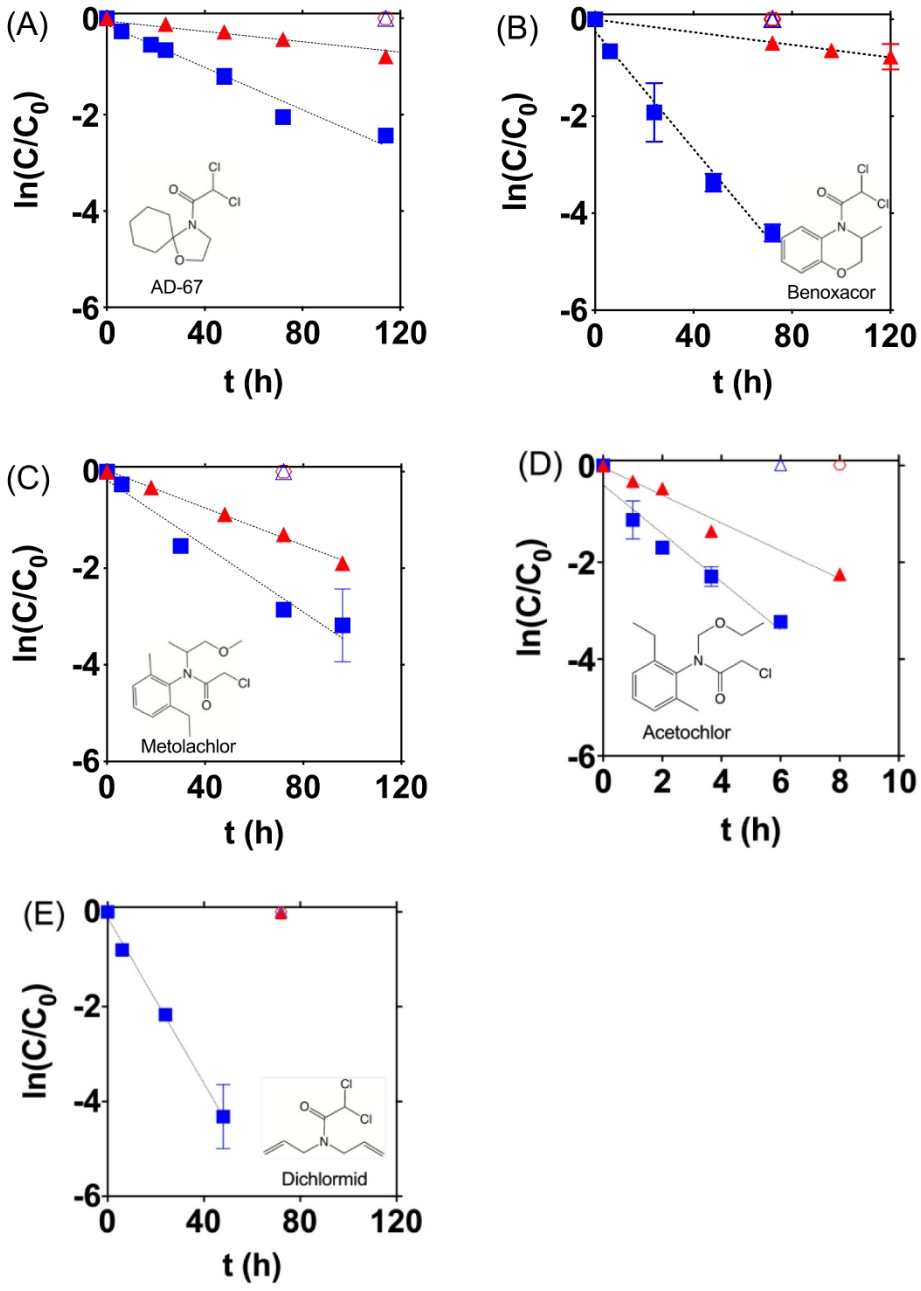

Fig. 1. Degradation of (A) AD-67 ($C_0 = 21$ μM), (B) benoxacor ($C_0 = 24$ μM), (C) metolachlor ($C_0 = 28$ μM), (D) dichlormid ($C_0 = 26$ μM) and (E) acetochlor($C_0 = 22$ μM) by *TOT*HS with (■) or without (▲) graphite powder; ○=controls containing only graphite; △=controls contaning only MOPS buffer. Uniform conditions: $[TOTHS]_0 = 5$ mM, [graphite powder] = 21 g·L^{-1}, T = 25 °C, pH = 7.2 (10 mM MOPS buffer). Error bar represents the standard deviation of experimental duplicates.

chromatograms, and their mass spectra are summarized in Table S5, Figs. S5–S8, and S14, respectively. Notably, the products detected in the homogeneous system (*TOT*HS-only) were a subset of the products detected in the heterogeneous system containing graphite and *TOT*HS. It is possible that the additional products detected in the presence of graphite is due to faster reation kinetics compared to the homogeneous system. Alternatively, there might be other reaction pathway(s) in the heterogeneous system.

A previous study reported the formation of only mono-sulfur bridged dimers (*e.g.*, mercaptochloroacetanilides detected by GC–MS) during the transformation of metolachlor by bisulfide (Loch et al., 2002). However, our LC-MS analyses indicate the formation of multisulfur-bridged dimers in both heterogeneous and homogeneous systems. The discrepancy might be attributed to the different analytical methods applied in these studies. Specifically, the acidification and/or methylation applied in the GC–MS method of the previous study (Loch et al., 2002) could accelerate the dissociation of sulfur-bridged compounds (Kamyshny et al., 2007; Kristiana et al., 2010; Lippa and Roberts, 2002). In contrast, no chemical pre-treatment was applied for the LC-MS analysis. Moreover, the high temperature of the GC inlet and the higher energy of the electron ionization source (relative to electrospray ionization) could promote fragmentation of reaction products (Loch et al., 2002).

Overall, the transformation of (di)chloroacetamides by *TOT*HS in the absence or presence of graphite generated an array of sulfur-substituted products. Together with the release of chloride, these results suggest that transformation of (di)chloroacetamides followed a nucleophilic substitution pathway. Polymerization of (di)chloroacetamides is possible in the presence of *TOT*HS and graphite, which significantly increased the molecular weight of the transformation products and decreased

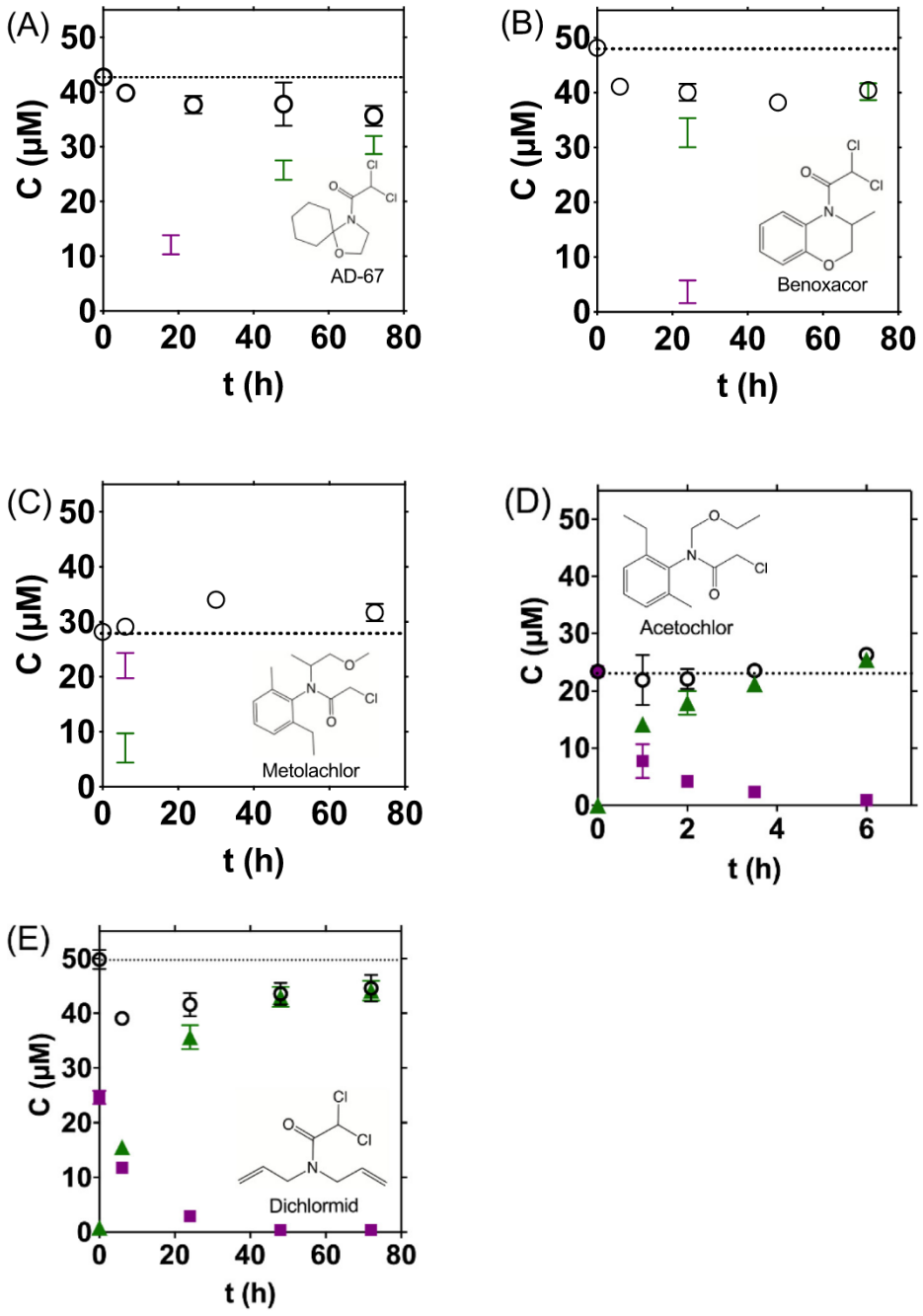

Fig. 2. Decay of (di)chloroacetamides (■) and the formation of chloride (▲) by 5 mM TOT*HS* in the presence of graphite powder (21 g·L^{-1}) for (A) AD-67 (C_0 = 21 μM), (B) benoxacor (C_0 = 24 μM), (C) metolachlor (C_0 = 28 μM), (D) dichlormid (C_0 = 26 μM) and (E) acetochlor (C_0 = 22 μM) ○=mass balance on the total chlorine, calculated as 2 [dichloroacetamide] + [monochloroacetamide] + [Cl^-]. Dashed line denotes the initial concentration of the total chlorine. All experiments were carried out at T = 25 °C and pH = 7.2 (10 mM MOPS); error bars represent the standard deviation of experimental duplicates.

their polarity as indicated by longer elution times for reversed-phase HPLC (Tables 1 and S5, Figs. S5–S8).

3.3. Examination of reaction pathways

Several reaction pathways can conceivably account for the observed synergistic effect between *TOT*HS and black carbon in promoting the tranformation of (di)chloroacetamides. Specifically, black carbon could: (I) facilitate electron transfer *via* its graphitic region from *TOT*HS to adsorbed (di)chloroacetamides and thus accelerate (di) chloroacetamide reduction (Xu et al., 2010); (II) react with *TOT*HS, forming a surface-bound nucleophile that subsequently attacks (di) chloroacetamides (Ding and Xu, 2016); and/or (III) oxidize *TOT*HS into reactive sulfur species, such as S_n^{2-}, which is more nucleophilic than HS^- during reactions with chloroacetamides (Lippa and Roberts, 2002; Loch et al., 2002). Notably, more than one of these pathways could occur concurrently.

To differentiate the contribution from each pathway, electrochemical cells were set up to quantify (di)chloroacetamide decay by pathway (I) alone. *TOT*HS-pretreated graphite systems were used to isolate pathway (II) (Ding and Xu, 2016; Xu et al., 2010). Batch reactors containing both graphite sheet and *TOT*HS were employed to encompass all three pathways. As shown in Fig. 3A, fast decay of (di)chloroacetamides occurred in batch reactors containing both graphite sheet and *TOT*HS, where 40 ± 9% of AD-67, 70 ± 3% of benoxacor, 30 ± 2% of dichlormid, and 60 ± 4% of metolachlor disappeared after 48 h, repectively; 77 ± 4%

of acetochlor disappeared after 6 h. Controls containing only graphite sheet showed no discernable decay of (di)chloroacetamides (Fig. S9). Degradation of all (di)chloroacetamides was negligible in both the electrochemical cells and *TOT*HS-pretreated graphite systems after 48 h. The reactivity seems to follow a different order using graphite powder and graphite sheet of similar properties: dichlormid is the most reactive using powder but the least using sheet. We suspect that the sorption process may play a role for such differences as the k_{obs} for (di) chloroacetamides are potentially influenced by three processes, namely, adsorption, surface reaction, and desorption. As shown in Fig. S4, the adsorption of dichlormid onto graphite sheet plateaued out in half an hour, while much faster adsorption was observed for graphite powder (<1 min). However, we do acknowledge that the reaction sites of black carbon may vary and the carbon type dependence requires further investigation. In contrast, over 99% of all (di)chloroacetamides disappeared in systems containing 300 μM S_n^{2-} together with 5 mM *TOT*HS and 1 mM S_8. Together, these results suggest that reduced sulfur species (S_n^{2-} or S_8) may play an important role in accelerating the decay of (di)chloroacetamides.

To confirm that pathway (I), namely reduction, was not responsible for the observed decay of (di)chloroacetamides, solutions of each (di) chloroacetamide (21–28 μM) were electrochemically reduced at E_H = −0.47 V. After 48 h, no decay of (di)chloroacetamides was observed (Fig. 3B), suggesting that the contribution of pathway (I) to the observed degradation of (di)chloroacetamides in batch reactors containing both graphite and *TOT*HS was negligible. Furthermore, the experimental set up of *TOT*HS-pretreated graphite systems as a means of isolating pathway (II) was validated using 1,1,1-trichloroethane as a positive control. A comparable amount of 1,1,1-trichloroethane decay (~50%) occurred after 48 h in batch reactors containing either graphite sheet + *TOT*HS or *TOT*HS-pretreated graphite (Fig. S10), suggesting that pathway (II), involving formation of a surface-bound sulfur nucleophile between graphite and *TOT*HS, was responsible for the observed decay of 1,1,1-trichloroethane but not (di)chloroacetamides. The observed differences between dichloroacetamides and 1,1,1-trichloroethane could be attributed to their distinctive chemical structures and the associated reaction pathways. For instance, the fact that dichloroacetamides have only two chlorine atoms and are alpha to an amide group likely drives the reactivity difference between dichloroacetamides and 1,1,1-trichloroethane. Collectively, these findings suggest that reaction pathway (III), involving production of reduced sulfur species (S_n^{2-} or S_8), might be important in accelerating (di)chloroacetamide decay.

To gain additional insight into the possible role of pathway (III), we monitored the production of S_n^{2-} and S_8 in batch reactors containing graphite and *TOT*HS. The concentrations of S_8 and S_n^{2-} plateaued after

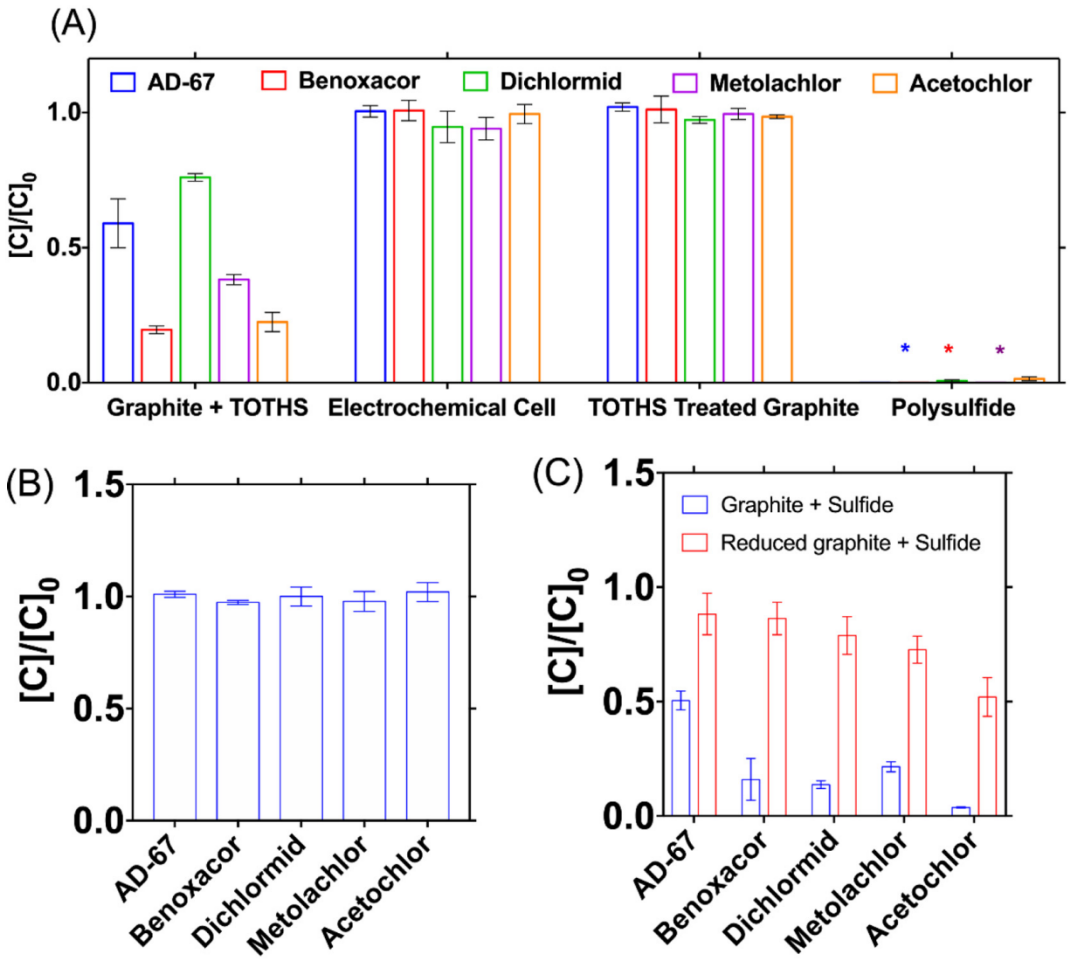

Fig. 3. (A) Degradation of (di)chloroacetamides in various reaction systems at pH 7.2 in 10 mM MOPS buffer after 48 h (6 h for acetochlor): Graphite + *TOT*HS (batch reactors containing 14 g·L^{-1} graphite sheet and 5 mM *TOT*HS); Electrochemical Cells (14 g·L^{-1} graphite sheet as the electrodes and 5 mM *TOT*HS in the anodic cell); *TOT*HS-pretreated Graphite (21 g·L^{-1} graphite powder was exposed to 5 mM *TOT*HS for 24 h and thoroughly rinsed to remove *TOT*HS residuals); and polysulfide (containing 5 mM *TOT*HS, 1 mM S_8, and 300 μM S_n^{2-}; concentrations of S_8 and S_n^{2-} were reported in sulfur atom); * denotes concentration below lowest point of standard curve (1 μM); (B) Direct electrochemical reduction of (di) chloroacetamides after 48 h (6 h for acetochlor) at pH 7.2 (10 mM phosphate buffer) with an applied potential of E_H = −0.47 V; (C) Degradation of (di)chloroacetamides by 5 mM TOTHS in the presence of electrochemically reduced or unmodified graphite powder (21 g·L^{-1}) at pH 7.2 (10 mM MOPS) after 48 h (6 h for acetochlor) The initial concentrations of (di)chloroacetamides are: $[AD\text{-}67]_0$ = 21 μM, $[benoxacor]_0$ = 24 μM, $[dichlormid]_0$ = 26 μM, $[metolachlor]_0$ = 28 μM, $[acetochlor]_0$ = 22 μM. Error bar represents the standard deviation of experimental duplicates.

several minutes at ~330 μM and ~ 300 μM, respectively (Fig. S10). Neither S_8 nor S_n^{2-} was detected in controls without graphite, suggesting that graphite significantly accelerated formation of S_8 and S_n^{2-}.The contribution of S_8 was further investigated by comparing the decay of (di) chloroacetamides in two systems: one containing *TOT*HS (no added S_8) and the other containing freshly prepared *TOT*HS and S_8 (Fig. S11), where generation of S_n^{2-} is expected to be negligible due to the slow kinetics under such conditions (Avetisyan et al., 2019). No discernable differences were observed between these systems, indicating that S_8 was not responsible for the enhanced decay of (di)chloroacetamides. Therefore, we postulate that S_n^{2-} contributed to the accelerated decay of (di) chloroacetamides in batch reactors containing both black carbon and *TOT*HS. The formation of S_n^{2-} can be ascribed to reaction between bisulfide and S_8 (Eq. (1)) (Avetisyan et al., 2019; Kamyshny et al., 2007) where S_8 is postulated to form from the oxidiation of *TOT*HS by black carbon.

$$HS^- + \frac{(n-1)}{8} S_8 \rightleftharpoons H^+ + {S_n}^{2-} \quad (1)$$

To test our hypothesis on the formation of S_n^{2-}, we conducted experiments where the EAC of black carbon (graphite powder) was depleted electrochemically. As shown in Fig. 3C, degradation of (di) chloroacetamides by *TOT*HS was significantly retarded in the presence of electrochemically-reduced graphite powder, where only 10 ± 9% of AD-67, 13 ± 6% of benoxacor, 19 ± 7% of dichlormid, and 24 ± 5% of metolachlor disappeared after 48 h, respectively; 48 ± 8% of acetochlor disappeared after 6 h. Meanwhile, 50 ± 4% of AD-67, 80 ± 7% of benoxacor, 85 ± 3% of dichlormid, 75 ± 4% of metolachlor, and 96 ± 2% of acetochlor was transformed by *TOT*HS in the presence of unmodified graphite. These results suggest that the EAC of black carbon might accelerate oxidation of *TOT*HS to S_8, which can react further with bisulfide to form S_n^{2-}. The formed S_n^{2-} likely accounts for the accelerated decay of (di)chloroacetamides in batch reactors containing black carbon and *TOT*HS. The reaction pathway is illustrated in Scheme S1 using dichlormid as an example. Notably, the products in such systems can be more complex than what is illustrated in Scheme S1. For instance, our LC-MS results indicate that dimeriazation and trimerization could occur through rearrangement of sulfur chains.

3.4. Degradation of dichlormid in the presence of biochar and TOTHS

To evaluate the feasilbity of using biochar to facilitate transformation of (di)chloroacetamides by *TOT*HS, a temperature series (400–700 °C) biochar was produced from wood feedstock. The chars are abbreviated as WX, where W refers to wood feedstock and X corresponds to the pyrolysis temperature. One of the dichloroacetamide safeners, dichlormid, was selected as the model pollutant because no aqueous-phase reaction with *TOT*HS was observed over 48 h. Therefore, degradation of dichlormid in batch reactors containing biochar and *TOT*HS ostensibly must result from reactions other than solution-phase reactions with *TOT*HS.

Similar to previous findings (Keiluweit et al., 2010; Klüpfel et al., 2014), the polarity of biochar decreased and its aromaticity increased with increasing pyrolysis temperature, as evidenced by the decreasing O/C and H/C ratios (Table S1). Conductivity of biochar increased as charring temperature increased (Table S1). EAC of biochar ($mmol_{e^-} \cdot g_{char}^{-1}$) was measured using a back titration method, where 400 °C char showed the highest EAC value. Degradation of dichlormid (Fig. 4A) by *TOT*HS occurred in the presence of all four biochars ($10\ g \cdot L^{-1}$), with observed rate constants decreasing in the order: 400 °C biochar (k_{obs} = 0.025 ± 0.003 h^{-1}) > 700 °C biochar (k_{obs} = 0.016 ± 0.004 h^{-1}) ≈ 600 °C biochar ($k_{obs} = 0.013 \pm 0.005\ h^{-1}$) ≈ 500 °C biochar ($k_{obs} = 0.012 \pm 0.002\ h^{-1}$). Controls without biochar showed negligible dichlormid decay.

To understand the properties of biochar that are important in accelerating dichlormid decay, correlation analyses were carried out between the obtained k_{obs} values and two biochar properties, namely, conductivity and EAC. No correlation between k_{obs} values for dichlormid decay and measured conductivity of biochar was observed. The least conductive biochar (W400) showed the highest reactivity, while the most conductive biochar (W700) showed relatively low reactivity (Fig. S13). In constract, decay rates of dichlorimid increased as the EAC values of biochar increased (Fig. 4A, $R^2 = 0.61$). Stronger correlations were obtained between k_{obs} values and the concentrations of S_8 (Fig. 4B, $R^2 = 0.98$) and S_n^{2-} (Fig. 4C, $R^2 = 0.98$), respectively, in batch reactors containing biochar and *TOT*HS. It appeared that as EAC values of biochar increased, the production of S_8 and S_n^{2-} increased, and the rates of dichlormid decay increased. These results suggest that decay of dichlormid in systems containing biochar and *TOT*HS might be attributed to oxidation of *TOT*HS to S_8 by the biochar with subsequent formation of S_n^{2-}.

Previous studies reported that the conductivity of black carbon was important in facilitating the decay of RDX and 2,4-dinitrotoluene by *TOT*HS (Oh et al., 2013; Xu et al., 2013). However, our results suggest that the EAC of biochar, rather than conductivity, played a predominant role in accelerating (di)chloroacetamide decay. The observed differences could result from differing reaction pathways and rate-limiting steps in contaminant decay. Specifically, we propose that nucleophilic substitution between S_n^{2-} and dichlormid, rather than formation of S_8, is rate-limiting. This is supported by the fast formation kinetics of S_8 (Fig. S10), where the concentration of S_8 plataued within several minutes. The EAC of biochar could arise from either surface quinones or condensed polyaromatic structures in high temperature biochars (Klüpfel et al., 2014), which can serve as electron acceptors during oxidation of *TOT*HS to S_8.

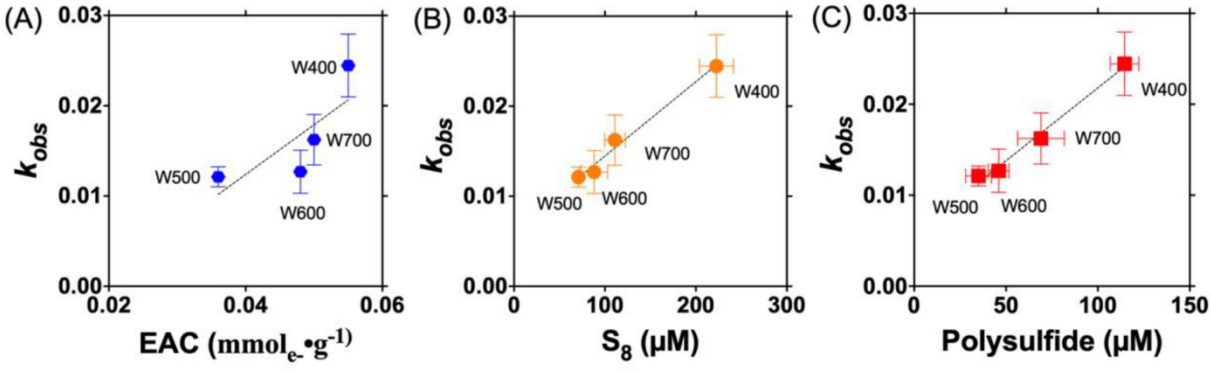

Fig. 4. The correlation analyses between the k_{obs} values of dichlormid (C_0 = 26 μM) and (A) measured EAC ($mmol_{e^-} \cdot g_{char}^{-1}$) of biochar; (B) concentrations of S_8; and (C) concentrations of S_n^{2-} in batch reactor containing $10\ g \cdot L^{-1}$ biochar and 5 mM *TOT*HS at pH 7 (10 mM MOPS buffer) at 25 °C; reaction time is 48 h. Error bar represents the standard deviation of experimental duplicates. The obtained linear regressions were: (A) $k_{obs} = (0.55 \pm 0.31) * EAC - (0.01 \pm 0.01)$, $R^2 = 0.61$; (B) $k_{obs} = (8.3 \pm 0.9) * 10^{-5} [S_8] - (0.006 \pm 0.001)$, $R^2 = 0.98$; (C) $k_{obs} = (1.6 \pm 0.1) * 10^{-4} [S_n^{2-}] - (0.005 \pm 0.001)$, $R^2 = 0.98$.

4. Conclusion

The reaction between reduced sulfur species (*e.g.*, bisulfide, S_8, and S_n^{2-}) and organic contaminants has received increasing attention in the environmental literature (Barbash and Reinhard, 1989; Butler and Hayes, 2000; Ding and Xu, 2016; Lippa and Roberts, 2002; Loch et al., 2002; Zhao et al., 2019; Zheng et al., 2006). This study, however, is one of few attempts to scrutinize the complexity of the associated reaction pathways. Firstly, we found that all three dichloroacetamide safeners and two chloroacetamide herbicides underwent rapid transformation when black carbon and *TOT*HS coexisted, generating an array of products, such as higher molecular weight (multi)sulfur-substituted products. The reaction pathway reported here is different from the Fe(II)-amended goethite system (Sivey and Roberts, 2012), where reductive dechlorination is responsible for safener decay. Nonetheless, the relatively rapid decay of safeners in both systems (*e.g.*, $t_{1/2}$ of 10 h for dichlormid by graphite-*TOT*HS *vs.* $t_{1/2}$ of 50 h by Fe(II)-amended goethite (Sivey and Roberts, 2012)) suggest that black carbon, *TOT*HS, and iron minerals could all be important in the subsurface environments. Reaction kinetics might be slower in natural systems given that the concentration of black carbon and minerals could vary to a large extent.

Some of the sulfur-substituted products here are less polar than their parent compounds and are therefore anticipated to be more readily sequestered (*e.g.*, through adsorption processes by soil particles) and, thus, less mobile and less bioavailable in aqueous systems relative to the parent compounds. Notably, the concentrations of dichloracetamide safeners are likely to be lower in natural systems (Wilson and James, 1987; Woodward et al., 2018) and the dimerization and trimeirization might proceed to a lesser extent. Nevertheless, black carbon may concentrate dichloroacetamide safeners and subsequently promote surface-mediated dimerization and trimerization. Moreover, the ubiquitous presence of natural organic matter (NOM) could affect the fate of safeners in the environment. For instance, it is possible that the sulfur-substituted products could form adducts with NOM that are anticipated to be less mobile than the parent dichloroacetamides. Furthermore, if sulfur-substituted products are transported to oxic environments, oxidation of these products is likely to occur and may generate products (*e.g.*, sulfonic acid derivatives) with higher water solubility (Aga and Thurman, 2001). Therefore, the possibility for further transformations and the associated end products, as well as their ecotoxicity, warrants further investigation.

Previous studies suggest that the synergistic effect between black carbon and *TOT*HS could be ascribed to the formation of surface-bound sulfur nucleophiles (Ding and Xu, 2016), electron transfer at graphitic regions (Xu et al., 2010) and/or polysulfide formation mediated by redox-active surface quinone groups (Zhao et al., 2019). The results of this study, however, suggest an additional (and previously unidentified) reaction pathway involving oxidation of *TOT*HS by black carbon, yielding reactive sulfur species that are responsible for the decay of (di)chloroacetamide. Specifically, black carbon was capable of oxidizing *TOT*HS to S_8, which led to the subsequent formation of S_n^{2-}. While this pathway could be limited by the finite EAC of black carbon, a replenishment of the EAC can occur during the anoxic-oxic regime shifts in the environment. The ubiqutious presence of *TOT*HS and black carbon in the subsurface environment suggests that this transformation pathway might influence the fate of contaminants other than (di)chloroacetamides; this possibility merits further research.

CRediT authorship contribution statement

Xiaolei Xu: Data curation, Formal analysis, Methodology, Writing - original draft.**John D. Sivey:**Formal analysis, Supervision, Writing - review & editing.**Wenqing Xu:**Project administration, Supervision, Writing - review & editing.

Declaration of competing interest

The authors declare that they have no known competing financial interests or personal relationships that could have appeared to influence the work reported in this paper.

Acknowledgement

X.X. and W.X. thank the U.S. National Science Foundation (NSF) CAREER award (CBET-1752220) for the financial support. J.D.S. acknowledges funding from the U.S. NSF (CBET-1703796 and CHE-1531562). Any opinions, findings, and conclusions or recommendations are those of the authors and do not necessarily reflect the views of the NSF. W.X. thanks the National Natural Science Foundation of China (No. 41728007) for travel support. X.X. and W.X. also acknowledge Drs. Charles Coe and Michale Smith at Villanova University for their help with BET surface measurements.

Appendix A. Supplementary data

Supplementary data to this article can be found online at https://doi.org/10.1016/j.scitotenv.2020.139908.

References

Abu-Qare, A.W., Duncan, H.J., 2002. Herbicide safeners: uses, limitations, metabolism, and mechanisms of action. Chemosphere 48, 965–974.
Acharya, S.P., Weidhaas, J., 2018. Solubility, partitioning, oxidation and photodegradation of dichloroacetamide herbicide safeners, benoxacor and furilazole. Chemosphere 211, 1018–1024.
Aga, D.S., Thurman, E.M., 2001. Formation and transport of the sulfonic acid metabolites of alachlor and metolachlor in soil. Environmental Science & Technology 35, 2455–2460.
Aga, D.S., Thurman, E.M., Yockel, M.E., Zimmerman, L.R., Williams, T.D., 1996. Identification of a new sulfonic acid metabolite of metolachlor in soil. Environmental Science & Technology 30, 592–597.
Anslyn, E.V., Dougherty, D.A., 2005. Modern Physical Organic Chemistry. University Science: Sausalito, California.
Avetisyan, K., Buchshtav, T., Kamyshny, A., 2019. Kinetics and mechanism of polysulfides formation by a reaction between hydrogen sulfide and orthorhombic cyclooctasulfur. Geochim. Cosmochim. Acta 247, 96–105.
Barbash, J.E., Reinhard, M., 1989. Reactivity of sulfur nucleophiles toward halogenated organic compounds in natural waters. Biogenic Sulfur in the Environment 393, 101–138 American Chemical Society.
Bolyard, K., Gresens, S.E., Ricko, A.N., Sivey, J.D., Salice, C.J., 2017. Assessing the Toxicity of the "Inert" Safener Benoxacor toward *Chironomus riparius*: Effects of Agrochemical Mixtures. 36 pp. 2660–2670.
Butler, E.C., Hayes, K.F., 2000. Kinetics of the transformation of halogenated aliphatic compounds by iron sulfide. Environmental Science & Technology 34, 422–429.
Christian, S., Pradhan, P., Jans, U., 2018. Investigation of the nucleophilic attack of dichlorvos by reduced sulfur species using 1H NMR. J. Agric. Food Chem. 66, 424–431.
Cline, J.D., 1969. Spectrophotometric determination of hydrogen sulfide in natural waters. Limnology and Oceanography 14, 454–458. https://doi.org/10.4319/lo.1969.14.3.0454.
Coleman, S., Linderman, R., Hodgson, E., Rose, R.L., 2000. Comparative metabolism of chloroacetamide herbicides and selected metabolites in human and rat liver microsomes. Environ. Health Perspect. 108, 1151–1157.
Davies, J., Caseley, J.C., 1999. Herbicide Safeners: A Review. 55 pp. 1043–1058.
Ding, K., Xu, W., 2016. Black carbon facilitated dechlorination of DDT and its metabolites by sulfide. Environmental Science & Technology 50, 12976–12983.
Ding, K., Byrnes, C., Bridge, J., Grannas, A., Xu, W., 2018. Surface-promoted hydrolysis of 2,4,6-trinitrotoluene and 2,4-dinitroanisole on pyrogenic carbonaceous matter. Chemosphere 197, 603–610.
Dunnette, D.A., Chynoweth, D.P., Mancy, K.H., 1985. The source of hydrogen sulfide in anoxic sediment. Water Res. 19, 875–884.
European Chemicals Agency, 2020. European Chemicals Agency.
Feng, P.C.C., 1991. Soil transformation of acetochlor via glutathione conjugation. Pestic. Biochem. Physiol. 40, 136–142.
Goifman, A., Ryzkov, D., Gun, J., Kamyshny, A., Modestov, A., Lev, O., 2004. Inorganic polysulfides' quantitation by methyl iodide derivatization: Dimethylpolysulfide formation potential. Water Science and Technology 49, 179–184.
Hladik, M.L., Hsiao, J.J., Roberts, A.L., 2005. Are neutral chloroacetamide herbicide degradates of potential environmental concern? Analysis and occurrence in the upper Chesapeake Bay. Environmental Science & Technology 39, 6561–6574.
Hladik, M.L., Bouwer, E.J., Roberts, A.L., 2008. Neutral degradates of chloroacetamide herbicides: occurrence in drinking water and removal during conventional water treatment. Water Res. 42, 4905–4914.
Jablonkai, I., 2013. Herbicide Safeners: Effective tools to improve herbicide selectivity. In: Kelton, A.P.J. (Ed.), Herbicide-Current research and case studies in Use. InTech Publications.

Kale, V.M., Miranda, S.R., Wilbanks, M.S., Meyer, S.A., 2008. Comparative cytotoxicity of alachlor, acetochlor, and metolachlor herbicides in isolated rat and cryopreserved human hepatocytes. J. Biochem. Mol. Toxicol. 22, 41–50.
Kamyshny, A., Gun, J., Rizkov, D., Voitsekovski, T., Lev, O., 2007. Equilibrium distribution of polysulfide ions in aqueous solutions at different temperatures by rapid single phase derivatization. Environmental Science & Technology 41, 2395–2400.
Keiluweit, M., Kleber, M., 2009. Molecular-level interactions in soils and sediments: the role of aromatic π-systems. Environmental Science & Technology 43, 3421–3429.
Keiluweit, M., Nico, P.S., Johnson, M.G., Kleber, M., 2010. Dynamic molecular structure of plant biomass-derived black carbon (biochar). Environmental Science & Technology 44, 1247–1253.
Kemper, J.M., Ammar, E., Mitch, W.A., 2008. Abiotic degradation of hexahydro-1,3,5-trinitro-1,3,5-triazine in the presence of hydrogen sulfide and black carbon. Environmental Science & Technology 42, 2118–2123.
King, G.M., Klug, M.J., Wiegert, R.G., Chalmers, A.G., 1982. Relation of Soil Water Movement and Sulfide Concentration to *Spartina alterniflora* Production in a Georgia Salt Marsh. 218 pp. 61–63.
Klopman, G., Chakravarti, S.K., Harris, N., Ivanov, J., SaiakHov, R.D., 2003. In-Silico screening of high production volume chemicals for mutagenicity using the mcase QSAR expert system. SAR QSAR Environ. Res. 14, 165–180.
Klüpfel, L., Keiluweit, M., Kleber, M., Sander, M., 2014. Redox properties of plant biomass-derived black carbon (biochar). Environmental Science & Technology 48, 5601–5611.
Kolpin, D.W., Barbash, J.E., Gilliom, R.J., 1998. Occurrence of pesticides in shallow groundwater of the United States: initial results from the national water-quality assessment program. Environmental Science & Technology 32, 558–566.
Kral, A.E., Pflug, N.C., McFadden, M.E., LeFevre, G.H., Sivey, J.D., Cwiertny, D.M., 2019. Photochemical transformations of dichloroacetamide safeners. Environmental Science & Technology 53, 6738–6746.
Kristiana, I., Heitz, A., Joll, C., Sathasivan, A., 2010. Analysis of polysulfides in drinking water distribution systems using headspace solid-phase microextraction and gas chromatography–mass spectrometry. J. Chromatogr. A 1217, 5995–6001.
Li, Z., Mao, J., Chu, W., Xu, W., 2019. Probing the surface reactivity of pyrogenic carbonaceous material (PCM) through synthesis of PCM-like conjugated microporous polymers. Environmental Science & Technology 53, 7673–7682.
Lian, F., Xing, B., 2017. Black carbon (biochar) in water/soil environments: molecular structure, sorption, stability, and potential risk. Environmental Science & Technology 51, 13517–13532.
Lippa, K.A., Roberts, A.L., 2002. Nucleophilic aromatic substitution reactions of chloroazines with bisulfide (HS-) and polysulfides (Sn2-). Environmental Science & Technology 36, 2008–2018.
Lippa, K.A., Demel, S., Lau, I.H., Roberts, A.L., 2004. Kinetics and mechanism of the nucleophilic displacement reactions of chloroacetanilide herbicides: investigation of α-substituent effects. J. Agric. Food Chem. 52, 3010–3021.
Loch, A.R., Lippa, K.A., Carlson, D.L., Chin, Y.P., Traina, S.J., Roberts, A.L., 2002. Nucleophilic aliphatic substitution reactions of propachlor, alachlor, and metolachlor with bisulfide (HS-) and polysulfides (Sn2-). Environmental Science & Technology 36, 4065–4073.
Matsumura, Y., Takahashi, H., 1979. Potentiometric redox titration of quinone in carbon black with NaBH4 and I2. Carbon 17, 109–114.
McGuire, M.M., Hamers, R.J., 2000. Extraction and quantitative analysis of elemental sulfur from sulfide mineral surfaces by high-performance liquid chromatography. Environmental Science & Technology 34, 4651–4655.
Middelburg, J.J., Nieuwenhuize, J., van Breugel, P., 1999. Black carbon in marine sediments. Mar. Chem. 65, 245–252.
Moelwyn-Hughes, E.A., 1971. The Chemical Statics and Kinetics of Solutions. London. Academic Press, New York.
Mora, J.R., Cervantes, C., Marquez, E., 2018. New Insight into the Chloroacetanilide Herbicide Degradation Mechanism through a Nucleophilic Attack of Hydrogen Sulfide. 19 p. 2864.
Oh, S.-Y., Son, J.-G., Hur, S.H., Chung, J.S., Chiu, P.C., 2013. Black Carbon–Mediated Reduction of 2,4-Dinitrotoluene by Dithiothreitol. 42 pp. 815–821.
Pignatello, J.J., Mitch, W.A., Xu, W., 2017. Activity and reactivity of pyrogenic carbonaceous matter toward organic compounds. Environmental Science & Technology 51, 8893–8908.
Rosinger, Chris, Bartsch, Klaus, Schulte, Wolfgang, 2011. Safeners for Herbicides. In: Krämer, Wolfgang, Schirmer, Ulrich, Jeschke, Peter, Witschel, Matthias (Eds.), Modern Crop Protection Compounds, 2nd 3. Wiley-VCH, pp. 259–281.
Saburo, N., 1952. On the electronic structure of the carbonyl and the amide groups. Bull. Chem. Soc. Jpn. 25, 164–168.
Scarponi, L., Perucci, P., Martientti, L., 1991. Conjugation of 2-chloroacetanilide herbicides with glutathione: role of molecular structures and of glutathione S-transferase enzymes. J. Agric. Food Chem. 39, 2010–2013.
Sivey, J.D., Lehmler, H.-J., Salice, C.J., Ricko, A.N., Cwiertny, D.M., 2015. Environmental fate and effects of dichloroacetamide herbicide safeners: "inert" yet biologically active agrochemical ingredients. Environmental Science & Technology Letters 2, 260–269.
Sivey, J.D., Roberts, A.L., 2012. Abiotic reduction reactions of dichloroacetamide safeners: transformations of "inert" agrochemical constituents. Environmental Science & Technology 46, 2187–2195.
Su, L., Caywood, L.M., Sivey, J.D., Dai, N., 2019. Sunlight photolysis of safener benoxacor and herbicide metolachlor as mixtures on simulated soil surfaces. Environmental Science & Technology 53, 6784–6793.
US EPA, 2020. Overview of the Ecological Risk Assessment Process in the Office of Pesticide Programs.
Wilson, R.G., James, E.R., 1987. Degradation of dichlormid and dietholate in soils with prior EPTC, butylate, dichlormid, and dietholate exposure. Weed Sci. 35, 289–294.
Woodward, E.E., Hladik, M.L., Kolpin, D.W., 2018. Occurrence of dichloroacetamide herbicide safeners and co-applied herbicides in Midwestern U.S. streams. Environmental Science & Technology Letters 5, 3–8.
Wu, T., Gan, Q., Jans, U., 2006. Nucleophilic substitution of phosphorothionate ester pesticides with bisulfide (HS-) and polysulfides (Sn2-). Environmental Science & Technology 40, 5428–5434.
Xu, W., Dana, K.E., Mitch, W.A., 2010. Black carbon-mediated destruction of nitroglycerin and RDX by hydrogen sulfide. Environmental Science & Technology 44, 6409–6415.
Xu, W., Pignatello, J.J., Mitch, W.A., 2013. Role of black carbon electrical conductivity in mediating hexahydro-1,3,5-trinitro-1,3,5-triazine (RDX) transformation on carbon surfaces by sulfides. Environmental Science & Technology 47, 7129–7136.
Xu, W., Pignatello, J.J., Mitch, W.A., 2015. Reduction of nitroaromatics sorbed to black carbon by direct reaction with sorbed sulfides. Environmental Science & Technology 49, 3419–3426.
Zeng, T., Ziegelgruber, K.L., Chin, Y.-P., Arnold, W.A., 2011. Pesticide processing potential in prairie pothole porewaters. Environmental Science & Technology 45, 6814–6822.
Zeng, T., Arnold, W.A., Toner, B.M., 2013. Microscale characterization of sulfur speciation in lake sediments. Environmental Science & Technology 47, 1287–1296.
Zhao, H.-Q., Huang, S.-Q., Xu, W.-Q., Wang, Y.-R., Wang, Y.-X., He, C.-S., et al., 2019. Undiscovered mechanism for pyrogenic carbonaceous matter-mediated abiotic transformation of Azo dyes by sulfide. Environmental Science & Technology 53, 4397–4405.
Zheng, W., Yates, S.R., Papiernik, S.K., Guo, M., Gan, J., 2006. Dechlorination of chloropicrin and 1,3-dichloropropene by hydrogen sulfide species: redox and nucleophilic substitution reactions. J. Agric. Food Chem. 54, 2280–2287.
Zheng, D., Zhang, X., Li, C., McKinnon, M.E., Sadok, R.G., Qu, D., et al., 2015. Quantitative Chromatographic Determination of Dissolved Elemental Sulfur in the Non-aqueous Electrolyte for Lithium-Sulfur Batteries. 162 pp. A203–A206.